

SEISMIC PERFORMANCE AND DESIGN OF PRECAST CONCRETE SHEAR WALL STRUCTURAL SYSTEMS

Shana Kareem YALDKO¹, Zeki HASGUR²

¹Civil Engineering, Altınbaş University, Istanbul, Türkiye, Shanayaldiko04@gmail.com

(<https://orcid.org/0009-0004-1529-1194/>)

²Civil Engineering, Altınbaş University, Istanbul, Türkiye, zeki.hasgur@altinbas.edu.tr

(<https://orcid.org/0000-0002-7769-5678/>)

Received: 11.03.2023

Accepted: 26.02.2024

Published: 30.06.2024

*Corresponding author

Research Article

pp.53-69

DOI: 10.53600/ajesa.1263669

Abstract

Our understanding of the seismic behavior and constraints of reinforced concrete shear walls was to be improved by this work. The Alto Rio building's collapse as a consequence of an earthquake was evaluated in the first section. The second section made use of information from a three-dimensional seismic simulation test on a four-story, precast post-tensioned concrete shear wall structure that was built to scale. The aim was to create useful structural engineering models, perform analytical simulations to verify the structural models' capacity to mimic behaviors that are significant to structural engineers, and determine whether the analysis tools now available are enough to represent dynamic behavior.

Keywords: Seismic behaviour, Earthquake, Structural Engineering.

PREKAST BETON PERDE YAPI SİSTEMLERİNİN SİSMİK PERFORMANSI VE TASARIMI

Özet

Bu çalışma ile betonarme perde duvarların sismik davranışı ve kısıtlamaları hakkındaki anlayışımız geliştirilecektir. Alto Rio binasının deprem sonucu çökmesi birinci bölümde değerlendirilmiştir. İkinci bölüm, ölçekli olarak inşa edilmiş dört katlı, prekast ardgermeli beton perde duvar yapısı üzerindeki üç boyutlu sismik simülasyon testinden elde edilen bilgileri kullanmıştır. Amaç, faydalı yapısal mühendislik modelleri oluşturmak, yapısal modellerin yapısal mühendisler için önemli olan davranışları taklit etme kapasitesini doğrulamak için analitik simülasyonlar gerçekleştirmek ve şu anda mevcut olan analiz araçlarının dinamik davranışı temsil etmek için yeterli olup olmadığını belirlemektir.

Keywords: Sismik Davranış, Deprem, Yapı Mühendisliği.

1. Introduction

Concrete is extensively utilized in buildings and constructions as a structural material. The materials of concrete which are easily accessible, processed, cast and cost-effective as well as the high compressive strength have been commonly picked for the production (Ujianto et al., 2019). The strength of the concrete depends on the quantity and type of its components. Concrete created by a group of the main components (cement, sand, coarse, split and water) (Singh et al., 2015). Concrete fly ash mixture is usually utilized in concrete for high strength purposes. The geopolymers of high strength concrete are activated with sodium silicate and sodium hydroxide (Mohd Ali and Sanjayan 2016)(Wallace and Moehle 1993).

In the construction sector, the precast concrete industrial construction system is the rapid building method. This works on the rapid development of the construction industry, especially as it encourages the manufacture of housing and

facilities. Precast concrete structures are a branch of structural concrete. Precast concrete is poured under well controlled and manufactured conditions in the factory and subsequently assembled on the job site (Sørensen, 2018). After the items are cast, they are not moved and fixed on site until they are fully cured and solidified. Although the precast method is used for buildings or bridges in most cases, it is a method applicable to any type of structure and perhaps in combination with existing in-situ casting technique (Welp 1988).

1.1. Research Problem and Scopes

The study represents a comparative study of the results of a group of previous studies to find out the efficiency, effectiveness and accuracy of the seismic performance representation process and the design of the structural systems of the prefabricated concrete shear wall through the digital model or the numerical model. , and it was divided into three parts as follows:

- 1) The study examines the fall of the Alto Rio skyscraper following the 2010 Chilean earthquake. It uses structural analysis to evaluate alternative explanations for the collapse. The outcomes of studies and failures reveal specifics about the failure mechanism and point out places where design and detailing procedures may be strengthened. The strengths and weaknesses of the studies to pinpoint specifics of the failure mechanism are themselves significant findings of the study(Date 2014).
- 2) This study investigates the behavior of a post-tensioned, unbonded building model that was shaken by an E-Defense shaking table. It creates useful structural engineering models to use in analytical simulations to test how well they can replicate behaviours that are significant to structural engineers and to determine whether the analysis tools at hand are adequate to model the dynamic behaviour that emerges when a full-scale PT shear wall building is subjected to realistic earthquake ground shaking. The measured response data from the test helps to increase the performance expectations and present design concepts(Wang 2022)(Parra and Moehle 2014).
- 3) A new precast self-centering rocking shear wall system (PSCRSW) is proposed to enhance the seismic resilience of steel moment resisting frame (SMRF). The mechanical behavior of PDSFD was investigated and simulated, and the hysteretic performance under different design parameters was discussed and compared with that of the conventional shear wall. Design principles and suggestions for PSCRSW were given, and an efficient seismic resilient design method for enhancement of SMRF was proposed. Reliable numerical models for the prototype and the enhanced SMRF were established, and nonlinear dynamic analyses were performed to assess the effectiveness of enhancing strategy(Magna and Kunnath 2012)(Panagiotou, Kim, and Barbosa 2009).

1.2. Objective of Research

We can summarize the objectives of research as follows:

- 1) Practices.

- 2) Strengthening structures that are not seismically studied in a highly efficient manner by adding precast shear walls, thus preventing building daytime and reducing the damage caused by earthquakes.
- 3) To Study the designs of precast shear walls that have been subjected to a number of serious damages and earthquakes.

2. Model

2.1. PSCRSW Model

The seismic robust precast rocking shear wall that the authors invented includes the suggested PSCRSW (Lu and Panagiotou 2014), which is primarily made up of a precast reinforced concrete (RC) wall, a V-shaped steel bracing, and a pre-pressed disc spring friction damper (PDSFD), as shown in Figure (1). The embedded steel beam and V-shaped steel brace anchor the precast wall to the bottom wall or the foundation, and two PDSFDs are fitted at the two wall toes, respectively. With the intention of solely performing axial work, PDSFD should be pin linked to the wall. When there is lateral stress, the precast wall shakes around the pinned connection, and PDSFD is supposed to offer lateral resistance, self-centering ability, and energy dissipation ability (Maruta and Hamada 2010).

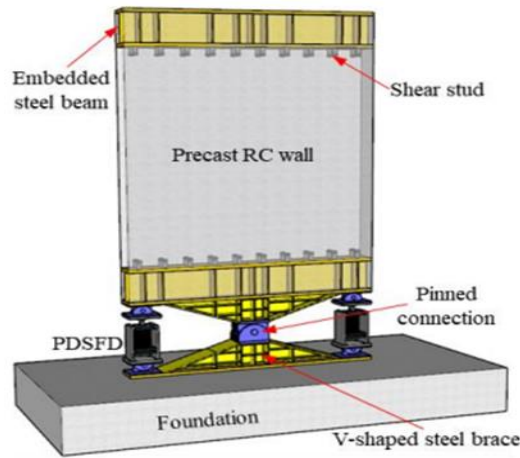


Figure 1: PDSFD schematic diagram.

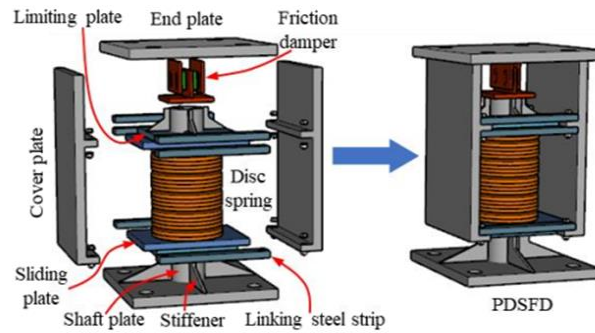


Figure 2: Schematic diagram of PDSFD

2.2. Software Model

An actual, four-story, post-tensioned precast concrete structure served as the test specimen. With dimensions of 14.4 m in X (longitudinal direction) and 7.2 m in Y (transverse direction), it featured a rectangular plan (Fig. 3). Each level was 3 m tall, giving the structure a total height of 12 m. Two precast unbounded PT shear walls and one bay unbounded PT center frame B axis made up the lateral-load-resisting system in the Y direction. The structural system in the X direction was made up of two bay-bonded PT frames. All structural components were prefabricated off-site, placed on-site, and then post-tensioned. After installation, grouting was used to join the post-tensioning tendons of the beams and columns in the X direction. However, shear wall and beam PT tendons in the Y direction were built to be unbounded from concrete (Balkaya and Kalkan 2003) (Vulcano, Bertero, and Colotti 1988).

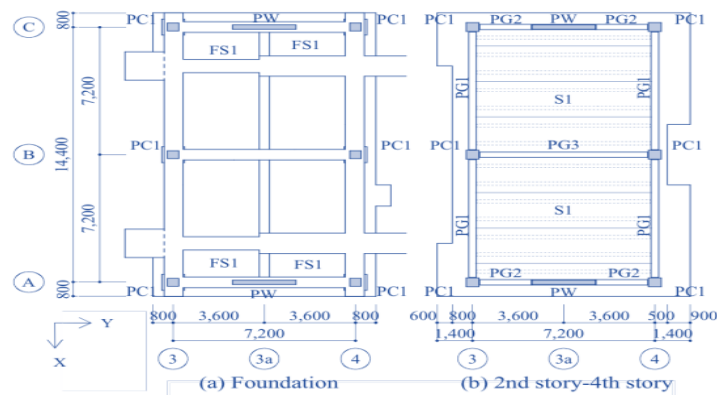


Figure 3: Floor plan of the specimen (Unit: mm)

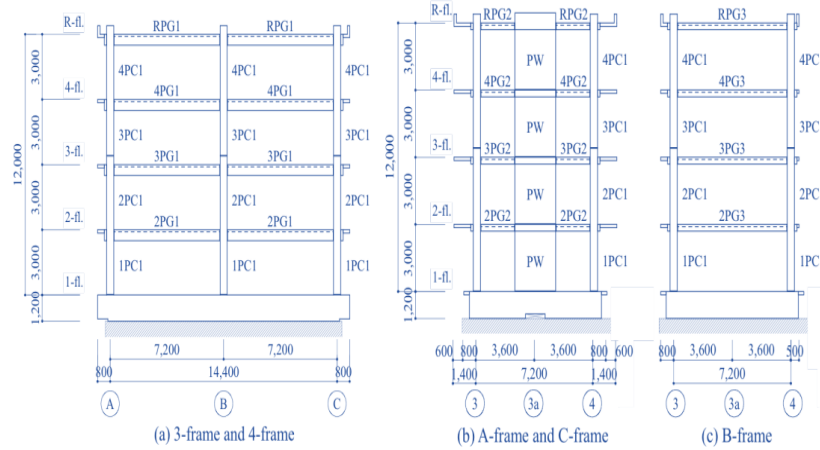


Figure 4: Elevation view of the specimen (Unit: mm)

Shearwalls had a rectangular cross-section that was 2500 mm in length and 250 mm in thickness. PT walls had a slenderness ratio of $H_w/l_w = 4.8$ due to their 12 m height. Square columns (PC1) had dimensions of 450 mm by 450 mm. The top 100 mm of the 300 mm by 300 mm portion of the beams (PG2 & PG3) was cast in situ at the same time as the slab. The top 100 mm of the slab's 130 mm thickness were cast monolithically on site with the beams. Pretensioned joists spaced 1 m apart in the transverse direction served as the slab's support. For further information, refer to Figure (5) (Wada et al. 2006).

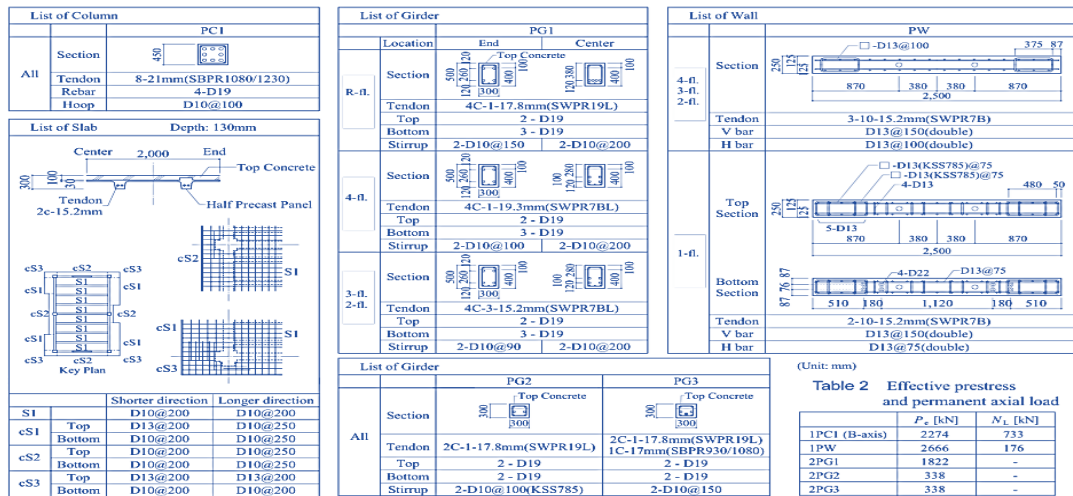


Figure 5: Member Cross-sections

Figure (6) depicts the wall-to-beam junction details and PT wall reinforcement features. Eight D22 (22 mm diameter) energy dissipation bars were unbonded across the bottom 1.5 meters of the first floor and mechanically coupled to the foundation. For walls and PG2 beams, the effective prestressing of the PT tendon was 0.6 times the yield strength; for the other beams and columns, it was 0.8 times the yield strength (Cement 1976).

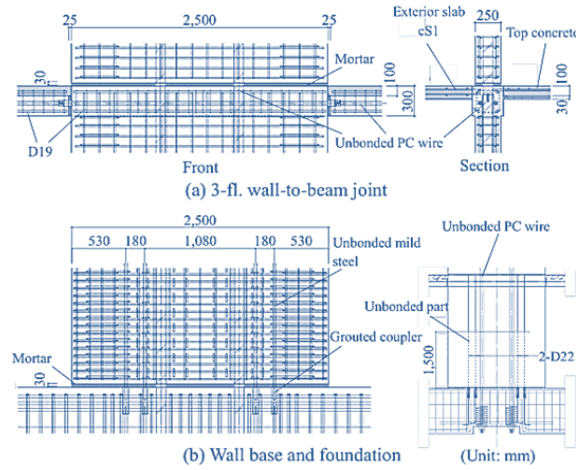


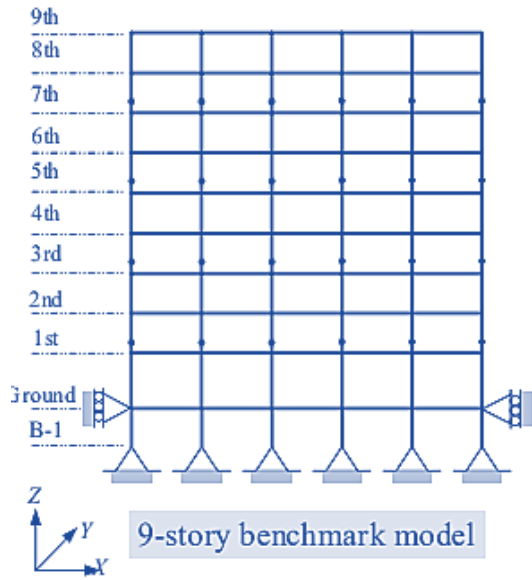
Figure 6: Reinforcement Details of Walls (Unit: mm)

The total weight of the specimen was 5592 kN. The weight of each floor was 996 kN for Roof, 813 kN for 3rd floor, 806 kN for 2nd floor and 804 kN for the 1st floor.

3. Case Study

3.1. Prototype Building

A typical 9-story SMRF that was originally created for the SAC project as the benchmark model and is frequently chosen to evaluate the effectiveness of seismic enhancing strategy was chosen as the prototype to be enhanced. The prototype is assumed to be located in Baghdad with a site class C, and the building has five bays that are 9.15 meters wide in each direction. Due to the structural symmetry, only one lateral resisting frame was studied in this work. The elevation view of the chosen frame and the member design details are shown in Figure 3.16. The height of the first level was 5.49 m, 3.65 m for the basement, and 3.96 m for the standard floor. W-section steel was used to make every member, having a nominal yield strength of 248 MPa for the beams and 345 MPa for the columns. Pins held the columns to the base together. The selected lateral resisting frame's tributary seismic mass was 4.50×106 kg.



| Beams (248 Mpa) | | Columns (345 Mpa) | | |
|-----------------------------------|--------------------|----------------------------------|----------|----------|
| Ground-2 nd | W36×160 | B-1-1 st | W14×1500 | |
| 3 rd – 6 th | W36×135 | 2 nd -3 rd | | |
| | W14×455 | 4 th -5 th | | |
| 7 th | W30×99 | 6 th -7 th | | |
| | W14×370 | 8 th -9 th | | |
| 8 th | W27×84 | | | |
| | W14×283 | | | |
| 9 th | W24×68 | | | |
| | W14×257 | | | |
| Weight | | Height | | Periods |
| Ground | 4.83×10^5 | Basement | 3.65 | |
| 1 st | 5.05×10^5 | 1 st | 5.50 | T1=2.05s |

Figure 7: Benchmark mode

3.2. Numerical Modeling

To account for the shear distortion effect, the trilinear hysteretic model developed by Gupta and Krawinkler (1999) was added into the rotating spring. The P-Δ effect was also considered in the numerical model by a leaning column that is built through a zero-length rotational spring with very small stiffness and rigid beam-column elements. The modeling of PSCRSW adopted a similar approach as illustrated in above. The only difference between them is that the RC wall is modeled using a beam-column element with a fiber section instead of a layered shell element. Each story wall was divided into four elements, and each element was assigned five integration points. Rigid links were established to connect the steel frame and PSCRSW. The detailed numerical model can be seen in Figure 8. Figure 9 compares the hysteretic curve of the wall specimen, simulated by fiber beam-column element, with that of the experiment and layered shell element-simulated model. As can be seen, the results are in good agreement with each other, indicating the effectiveness of the numerical model for PSCRSW.

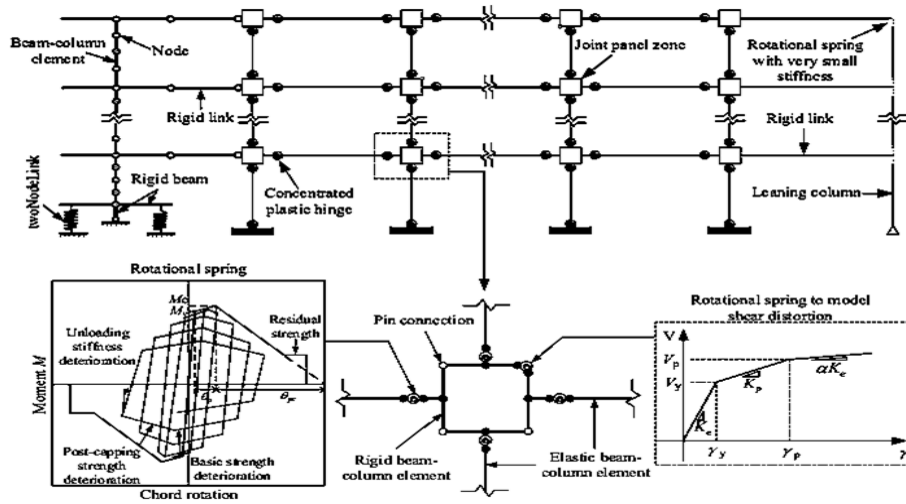


Figure 8: Numerical modeling for PSCRSW.

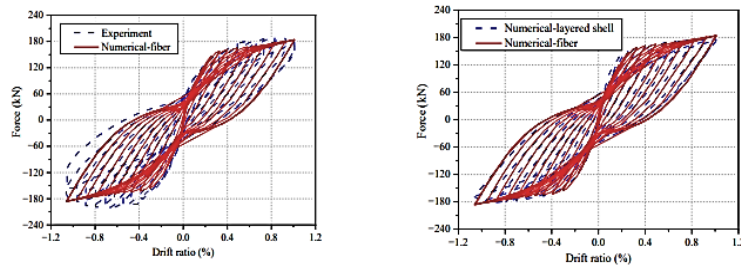


Figure 9: Hysteretic curve of the wall specimen simulated by fiber element.

3.3. Software Simulation

Utilizing the computer application Perform 3D, an analytical model in three dimensions of the specimen's Y direction was created (CSI). A 3D perspective of the model may be seen in Figure 3.19.

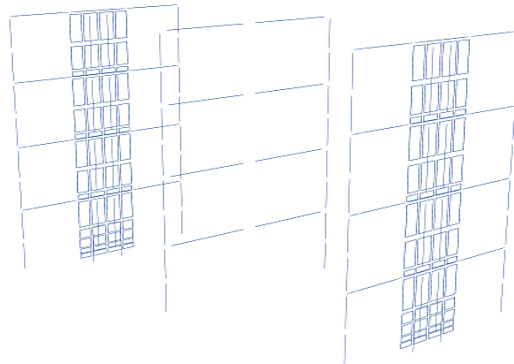


Figure 10: 3D view of the Perform 3D model.

4. Results And Discussion

4.1. Numerical Model Results

In this study, location = 0.4%, $0_d = 1.5\%$, and $1 = 2.0\%$ were chosen as the ISDR objectives for SLE, DBE, and MCE levels, respectively. In accordance with design step (3), a connection between inter-story and roof drift ratios was fitted using the prototype's dynamic reactions to the earthquake records presented in Section 4.4 as an excitation source. The results of the fitting are shown in Figure 15, and using these, it is possible to determine the roof drift ratio goals as 0.25%, 0.94%, and 1.25% for each seismic level. Then, in accordance with the design processes (4) through (6) stated in Table 4.1, further crucial design parameters can be determined. Design base shear was ultimately calculated to be 0.17W. The final period, 1.30 s, was close to the 1.34 s amount that was originally intended. It should be emphasized that the design was completed with just one loop and no iterations.

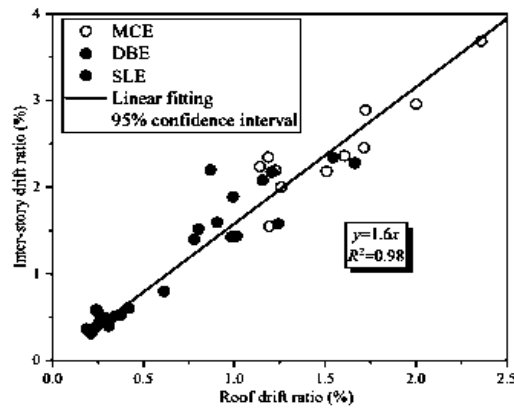


Figure 11: Fitting relationship between inter-story and roof drift ratios

Table 1: Parameters of Numerical Method

| Parameters | SLE | DBE | MCE |
|------------------------------|-------|--------|-------|
| T/s | 1.35 | 1.35 | 1.35 |
| Sa/G | 0.15 | 0.50 | 0.85 |
| $\theta_y \theta_d \theta_u$ | 0.5 % | 1.75 % | 2.0% |
| θ_p | 0 | 0.70 % | 1.0 % |
| μ_s | 1 | 3.75 | 5 |
| C_0 | 1.5 | 1.5 | 1.5 |
| γ | 1.0 | 0.50 | 0.30 |
| V_y/W | 0.10 | 0.10 | 0.15 |

The parameters in design step (7) were calculated, including $q = 543.8 \text{ kN/m}$, $CF = 7.53 \times 10^5 \text{ kN}$, $\lambda = 1.25$, $I_{eq} = 22.2 \text{ m}^4$. The material properties of the concrete and reinforcement were assumed to be the same, and the elastic modulus of concrete was $E_c = 3 \times 10^4 \text{ MPa}$. The dimensions of the wall section were computed as $L = 6.0 \text{ m}$, $t = 1.2 \text{ m}$, and the width of confined regions was selected as 0.8 m . The geometric parameters were assumed as $a = h' = 2.0 \text{ m}$ and $b = 0.3 \text{ m}$. The value of $p_0 + f_0$, k_1 and k_2 for PDSFD were calculated as $2.82 \times 10^4 \text{ kN}$, $4.18 \times 10^3 \text{ kN/mm}$ and $2.09 \times 10^2 \text{ kN/mm}$, respectively.

The inter-story drift ratio (ISDR) of the prototype and upgraded SMRF is distributed story-wise in Figure 4.4. The prototype's highest mean ISDRs, which are higher than the design goals, were 0.50%, 1.64%, and 2.30% at SLE, DBE, and MCE levels, respectively. The maximum ISDRs were decreased to 0.38%, 1.32%, and 1.99% after being improved. The roof drift ratios between the analytical values and the objectives are compared in Figure 15. The mean roof drift ratios were 0.25 percent, 0.8 percent, 1.3 percent, and 5%, showing the efficiency of the improved SMRF in achieving the anticipated seismic performance goals and the suggested design approach.

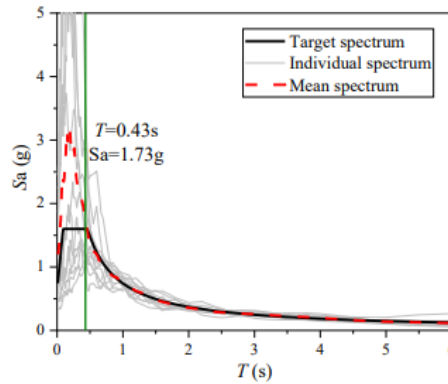


Figure 12: Response spectra of the earthquake records scaled to DBE level.

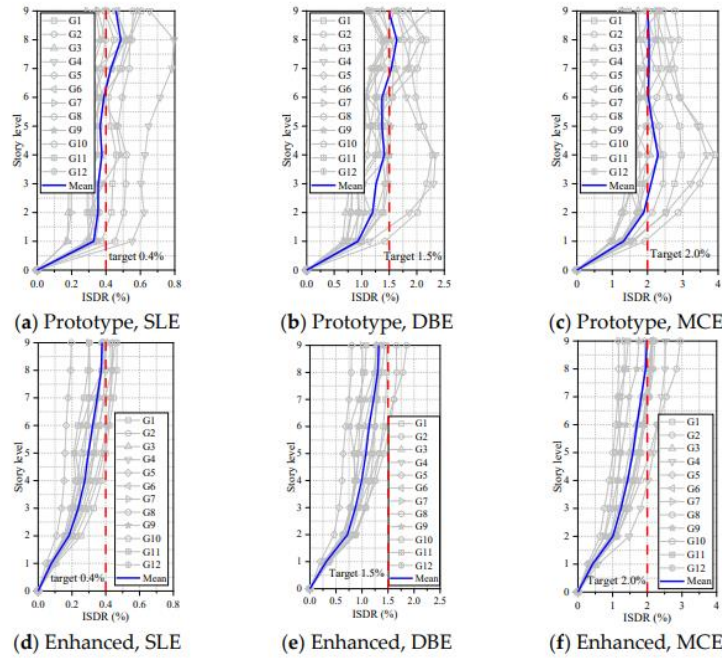


Figure 13: Inter-story drift ratio of the prototype and the enhanced SMRF. Inter-story drift ratio of the prototype and the enhanced SMRF.

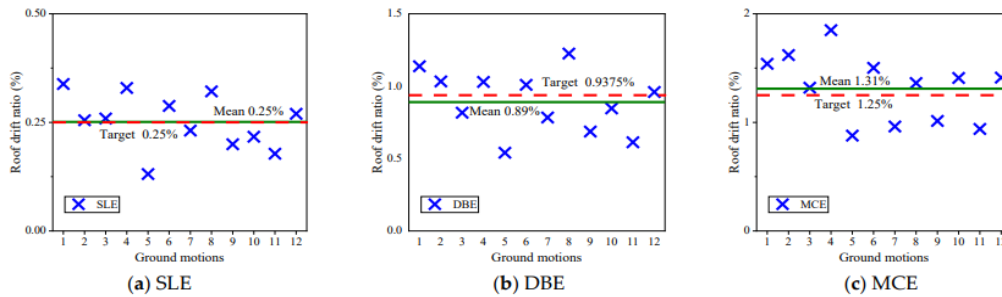


Figure 14: Comparison of the analytical and designed roof drift ratios.

Figure (15) shows the prototype and modified SMRF's roof drift time history curves using the reactions to earthquakes GM4 (with the greatest response) and GM5 (with the minimum response). Peak roof drifts are reduced by 122 mm, 383 mm, and 687 mm under the excitation of GM4, but residual drifts are decreased by 1.12 mm, 200 mm, and 461 mm to 0.02 mm, 13 mm, and 210 mm. The greatest residual inter-story drift ratios before and after augmentation are shown in Figure 20. The structural recoverability post-earthquakes would be severely reduced by the provided PSCRSW, since the average deterioration of all earthquake records is 54%.

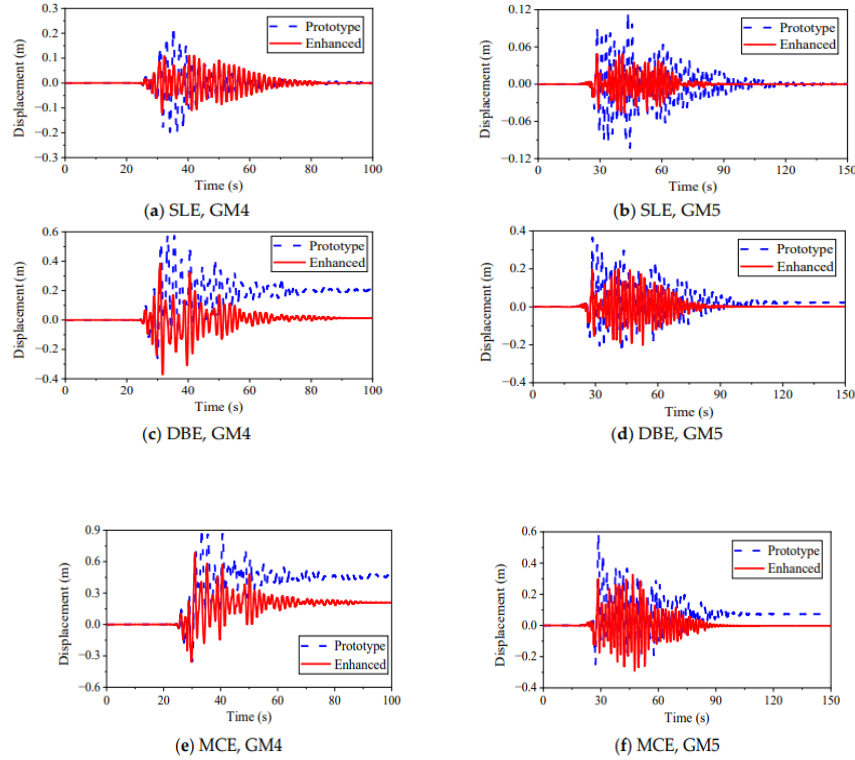


Figure (15): Comparison of the roof drift time history curves.

4.2. Comparison of Software Simulation and Numerical Analysis

Base shear versus roof drift ratio responses of the analytical model and test specimen under 25%, 50%, 100% Kobe excitations are shown in Figure 4.6, Figure 4.7, and Figure 4.8. Flag-shaped hysteresis typical of unbonded post-tensioned concrete is apparent, and initial stiffness does not match the test results. Maximum base shear is underestimated, and maximum roof drift ratio values are over-estimated except after 17 s of 100% Kobe motion. The contribution of the PT frames in the Y-direction may be significant and should be modeled for successful estimations of response. There is a good match of roof drift ratio versus time after 17 s, which could be a result of strength loss caused by heavy damage of the frames.

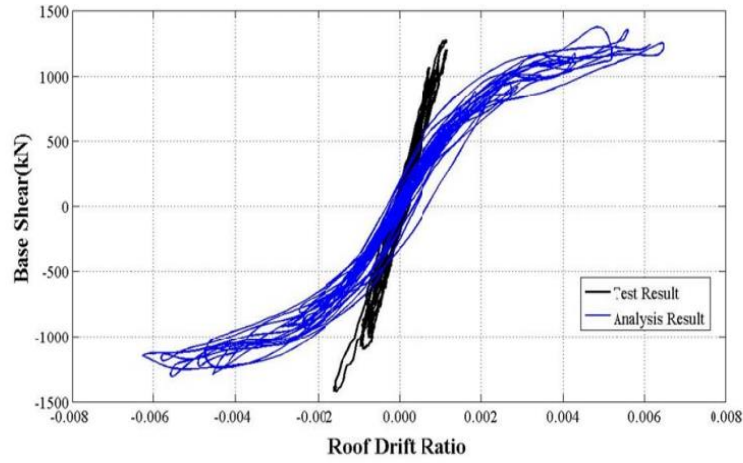


Figure 16: Base Shear-roof drift ratio comparison results for 25% Kobe motion.

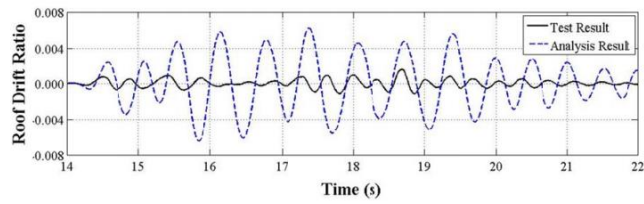


Figure 17: roof drift ratio comparison results for 25 % Kobe motion.

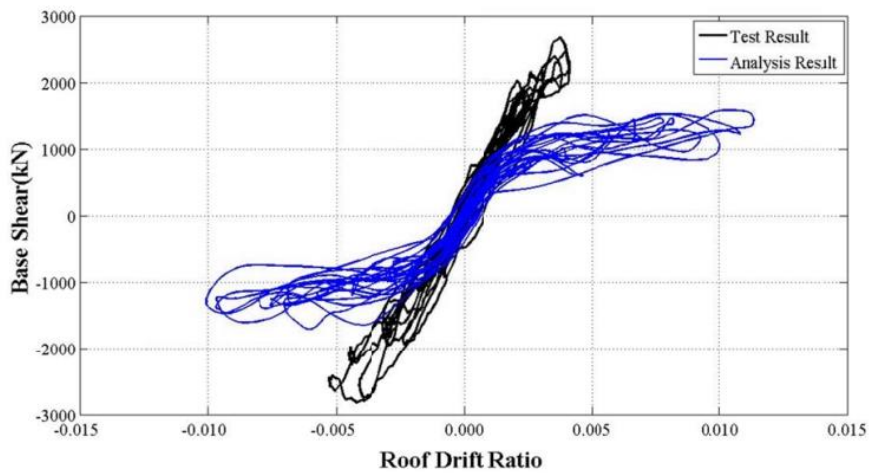


Figure 18: Base Shear-roof drift ratio comparison results for 50% Kobe motion.

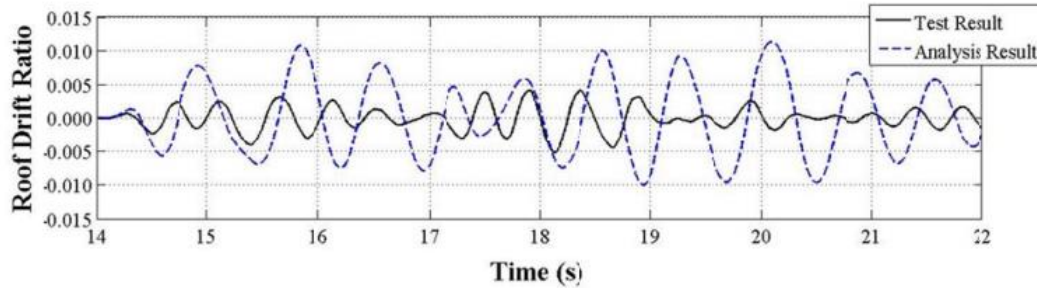


Figure 19: roof drift ratio comparison results for 50 % Kobe motion.

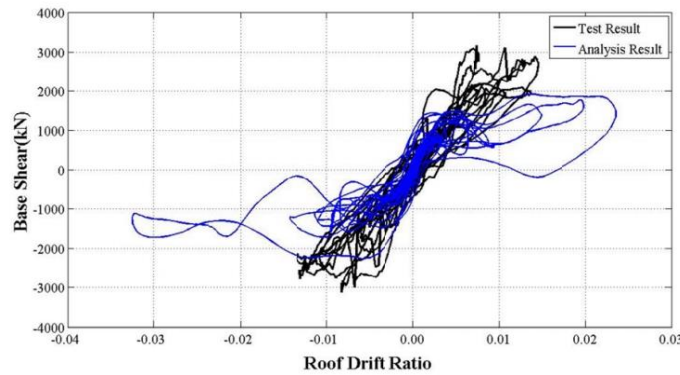


Figure 20: Base Shear-roof drift ratio comparison results for 100% Kobe motion.

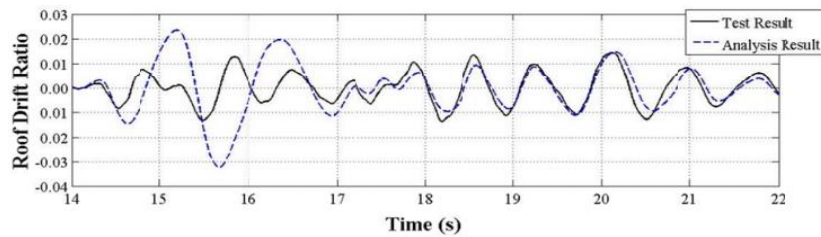


Figure 21: roof drift ratio comparison results for 100 % Kobe motion.

5. Conclusion

The following key findings and recommendations were attained by theoretical and numerical studies, which verified the effectiveness of the proposed PSCRSW and the design approach for increasing the seismic resistance of SMRF:

- 1) PSCRSW exhibits a stable flag-shaped hysteretic curve and approximate yielding behavior, displacement capacity, and lateral strength to the prototype (conventional RC shear wall). The ratio of preload P_0 to friction force f_0 of PSCRSW is recommended to be no less than 1.5 in order to ensure excellent self-centering performance;
- 2) When the ratio of P_0 to f_0 does not exceed 2.0, PSCRSW shows obviously better energy dissipation capacity than the prototype, with PDSFD dissipating about 70% of the energy. Additionally, the RC wall in PSCRSW dissipates more than 60% less energy than the prototype, indicating that the wall's plastic degradation in PSCRSW is significantly reduced;
- 3) When designing the PSCRSW, the RC wall's bearing capacity should take into account the amplification factor of 1.2, at which point not only the bearing performance but also the self-centering performance can be guaranteed;
- 4) Using the suggested design method, the enhanced SMRF meets the inter-story drift ratio targets and the anticipated roof drift ratios at the same time.
- 5) The seismic responses of the SMRF are greatly decreased after enhancement, with no iterations carried out throughout the enhancement design. By reducing the total energy lost by the beams and columns by 58% and 99%, respectively, and showing that the seismic resistance of SMRF is successfully increased by PSCRSW, the mean deterioration of residual inter-story drift ratios is around 54%.

References

- Balkaya, Can, and Erol Kalkan. 2003. "Nonlinear Seismic Response Evaluation of Tunnel Form Building Structures." *Computers and Structures* 81(3):153–65. doi: 10.1016/S0045-7949(02)00434-0.
- Cement, Portlan D. 1976. *PORTLAN'D CEMENT RILEY ASSOCIATION III EARTHQUAKE RESISTANT STRUCTURAL WALLS-TESTS OF ISOLATED WALLS NATIONAL TECHNICAL INFORMATION SERVICE*.
- Date, Publication. 2014. "UC Berkeley Electronic Theses and Dissertations Seismic Performance and Modeling of Reinforced Concrete and Post-Tensioned Precast Concrete Shear Walls."
- Lu, Yuan, and Marios Panagiotou. 2014. "Three-Dimensional Cyclic Beam-Truss Model for Nonplanar Reinforced Concrete Walls." *Journal of Structural Engineering* 140(3). doi: 10.1061/(asce)st.1943-541x.0000852.

Magna, C. E., and S. K. Kunnath. 2012. "Simulation of Nonlinear Seismic Response of Reinforced Concrete Structural Walls." *The 15th World Conference on Earthquake Engineering* (2006):1–10.

Maruta, Makoto, and Kimiya Hamada. 2010. "Shaking Table Tests on Three Story Precast Prestressed Concrete Frame." *Journal of Structural and Construction Engineering* 75(648):405–13. doi: 10.3130/aijs.75.405.

Mohd Ali, Ahmad Zurisman, and Jay Sanjayan. 2016. "The Spalling of Geopolymer High Strength Concrete Wall Panels and Cylinders under Hydrocarbon Fire." *MATEC Web of Conferences* 47:0–4. doi: 10.1051/mateconf/20164702005.

Panagiotou, Marios, Geonwoo Kim, and Andre Barbosa. 2009. "Response Verification of a Reinforced Concrete Bearing Wall Building Located in An Area of High Seismic Hazard." (Report No. SN2961).

Parra, P. F., and J. P. Moehle. 2014. "Lateral Buckling in Reinforced Concrete Walls." *NCEE 2014 - 10th U.S. National Conference on Earthquake Engineering: Frontiers of Earthquake Engineering* (August 2019). doi: 10.4231/D3V40K05Q.

Vulcano, A., Vitelmo V. Bertero, and Vincenzo Colotti. 1988. "Analytical Modeling of R/C Structural Walls." *9th World Conference on Earthquake Engineering* 41–44.

Wada, A., H. Sakata, K. Nakano, Y. Matsuzaki, K. Tanabe, and S. Machida. 2006. "Study on Damage Controlled Precast-Prestressed Concrete Structure with P / C MILD-PRESS-JOINT – Part 1 : Overview of P / C Mild-Press-Joint Building Construction and Its Practical Applications." *Proceedings of the 2nd Fib International Congress* 1:1–9.

Wallace, J. W., and J. P. Moehle. 1993. "An Evaluation of Ductility and Detailing Requirements of Bearing Wall Buildings Using Data from the March 3, 1985, Chile Earthquake." *Earthquake Spectra* 9(1):137–56. doi: 10.1193/1.1585709.

Wang, Zhiqi. 2022. "Structural Design and Seismic Analysis of Connecting Corridor in High-Rise Buildings."

Highlights in Science, Engineering and Technology 28:297–304. doi: 10.54097/hset.v28i.4161.

Welp, Katherine Marie. 1988. "Effective Stiffness of Rectangular Concrete Columns." (106):1–5.